Bioorganic & Medicinal Chemistry 20 (2012) 6513–6522

Contents lists available at SciVerse ScienceDirect

Bioorganic & Medicinal Chemistry

journal homepage: www.elsevier.com/locate/bmc

Novel multipotent phenylthiazole–tacrine hybrids for the inhibition of cholinesterase activity, β-amyloid aggregation and Ca^{2+} overload

Yue Wang [a], Fang Wang [a,d], Jun-Ping Yu [c], Feng-Chao Jiang [b], Xin-Lei Guan [a], Can-Ming Wang [a], Lei Li [b], Hui Cao [a], Ming-Xing Li [a], Jian-Guo Chen [a,d,*]

[a] Department of Pharmacology, Tongji Medical College, Huazhong University of Science and Technology, Wuhan, Hubei 430030, China
[b] Department of Medicinal Chemistry, Tongji Medical College, Huazhong University of Science and Technology, Wuhan, Hubei 430030, China
[c] State Key Laboratory of Virology, Wuhan Institute of Virology, Chinese Academy of Sciences, Wuhan, Hubei 430071, China
[d] The Key Laboratory for Drug Target Researches and Pharmacodynamic Evaluation of Hubei Province, Wuhan 430030, China

ARTICLE INFO

Article history:
Received 14 June 2012
Revised 9 August 2012
Accepted 10 August 2012
Available online 30 August 2012

Keywords:
Alzheimer's disease
Phenylthiazole–tacrine hybrids
Cholinesterase inhibition
β-Amyloid aggregation
Ca^{2+} overload

ABSTRACT

In this study, a series of multipotent phenylthiazole–tacrine hybrids (**7a**–**7e**, **8**, and **9a**–**9m**) were synthesized and biologically evaluated. Screening results showed that phenylthiazole–tacrine hybrids were potent cholinesterase inhibitors with pIC_{50} ($-\log IC_{50}$) value ranging from 5.78 ± 0.05 to 7.14 ± 0.01 for acetylcholinesterase (AChE), and from 5.75 ± 0.03 to 10.35 ± 0.15 for butyrylcholinesterase (BuChE). The second series of phenylthiazole–tacrine hybrids (**9a**–**9m**) could efficiently prevent $A\beta_{1-42}$ self-aggregation. The structure–activity relationship revealed that their inhibitory potency relied on the type of middle linker and substitutions at 4′-position of 4-phenyl-2-aminothiazole. In addition, **7a** and **7c** also displayed the Ca^{2+} overload blockade effect in the primary cultured cortical neurons. Consequently, these compounds emerged as promising molecules for the therapy of Alzheimer's disease.

1. Introduction

Alzheimer's disease (AD), the most common form of dementia in the elderly, is characterized by deposits of β-amyloid peptide (Aβ), neurofibrillary tangles, massive loss of neurons and severe cognition impairment.[1] Since cholinergic dysfunction contributes to the symptoms of AD patients, most of the commercialized drugs are mainly based on increasing cholinergic neurotransmission by inhibiting cholinesterase (doepenzil, rivastigmine, tacrine and galantanmine).[2]

An abnormal extracellular accumulation of β-amyloid peptides (Aβ) is another major neuropathological feature in AD. Aβ peptides are the main component of amyloid plaques and are accumulated through hydrolyzing Aβ precursor protein (APP) by β- and γ-secretase.[3,4] Aβ soluble oligomers and the assembly of Aβ aggregates into fibrils are toxic to neurons.[5] Compounds that are able to slow or block the Aβ polymerization process will serve as potential therapeutic drugs for AD treatment.[6]

AD is a multifaceted neurodegenerative disorder. It is unlikely that a unitary mechanism of action will provide a comprehensive therapeutic approach to such multifaceted neurodegenerative disease. Thus, efficient therapy is more likely to be achieved by drugs that incorporate several pharmacological effects into a single molecular entity.[7–9] Tacrine is the first approved cholinesterase inhibitor by the FDA. Although, its side effects, its modification is still of great interest.[10,11] Some multipotent compounds have been developed by conjugating tacrine with other active groups, such as acetylcholinesterase/β-amyloid-directed compounds (Fig. 1A and B),[12,13] dual-target inhibitors of cholinesterase/muscarinic M_1 receptors (Fig. 1C),[14] and dual-target inhibitors of cholinesterase/Ca^{2+} channels (Fig. 1D).[15,16]

Recently, it has been reported that phenylthiazolyl–hydrazide derivatives could block the pathological aggregation of tau protein and disturbed the formation of paired helical filaments (PHFs).[17,18] Given that the phenylthiazole scaffold could inhibit tau protein aggregation, we thought that its derivatives might also display pharmacological action on blockade of Aβ self-aggregation. In addition, phenylthiazole derivatives have attracted our interest because of their extensive biological actions, such as protecting neurons from ischemic damage and anti-inflammatory activity.[19–21] In this context, we designed and synthesized a series of novel multifunctional compounds by conjugating tacrine with 4-phenyl-2-aminothiazole group through different middle linkers (Fig. 2). The pharmacological effects of these novel compounds were investigated by measurement of acetylcholinesterase (AChE) and butyrylcholinesterase (BuChE) inhibition, $A\beta_{1-42}$

* Corresponding author. Tel.: +86 27 83692636; fax: +86 27 83692608.
E-mail address: chenj@mails.tjmu.edu.cn (J.-G. Chen).

0968-0896/$ - see front matter © 2012 Elsevier Ltd. All rights reserved.
http://dx.doi.org/10.1016/j.bmc.2012.08.040

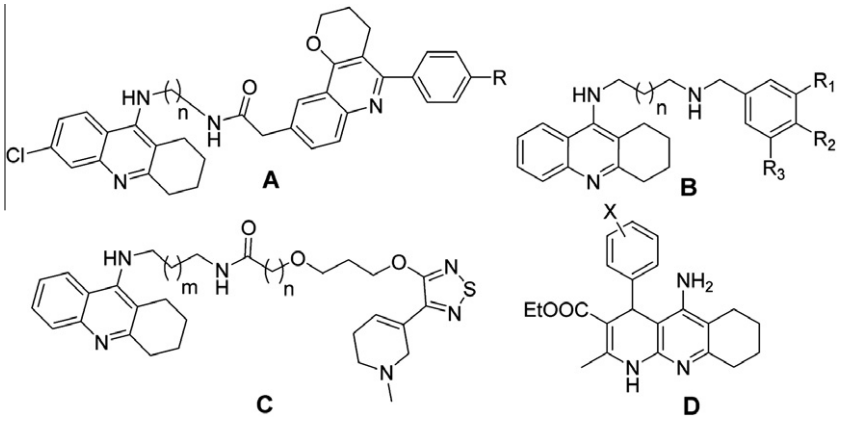

Figure 1. Multipotent tacrine derivatives.

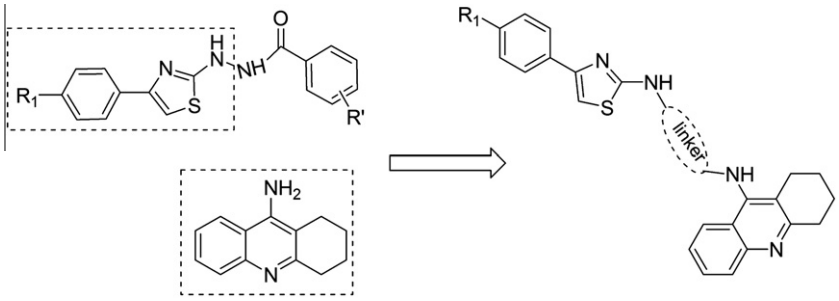

Figure 2. Design strategy of phenylthiazole–tacrine hybrids.

self-aggregation inhibitory activity, and Ca^{2+} overload blockade effect.

2. Results and discussion

2.1. Chemistry

The synthetic strategies to **7a**–**7e** and **8** were illustrated in Scheme 1. Intermediate **3a**–**3c** and **4** were prepared from 2-aminothiazole derivatives reacting with succinic anhydride or glutaric anhydride in THF. Intermediate **1** and **2** were synthesized according to the published method.[22] Reaction of **3a**–**3c** or **4** with **1** in the presence of 1-ethyl-3-(3-diethylaminopropyl) carbodiimide (EDC·HCl) and hydroxybenzotriazole (HOBt) in DMF/CH_2Cl_2 yielded compound **7a**–**7e** and **8**. Compound **9a**–**9m** were synthesized following the convergent synthetic approach in Scheme 2. 2-Aminothiazole derivatives reacted with chloroacetyl chloride or 3-bromopropionyl chloride to produce **5a**–**5f**. Reaction of **5a**–**5f**

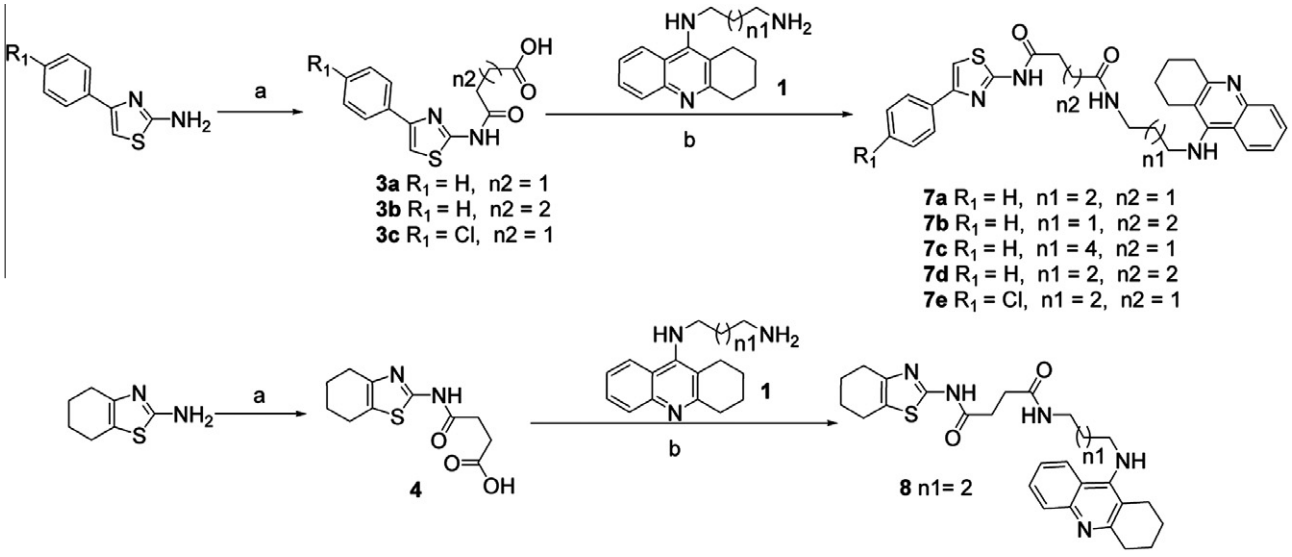

Scheme 1. Synthesis of the first series of phenylthiazole–tacrine hybrids (**7a**–**7e**, **8**). Reagents and conditions: (a) succinic anhydride or glutaric anhydride, THF, 65 °C, 7 h; (b) EDC·HCl/HOBt, DMF/CH_2Cl_2, 25 °C, 12 h.

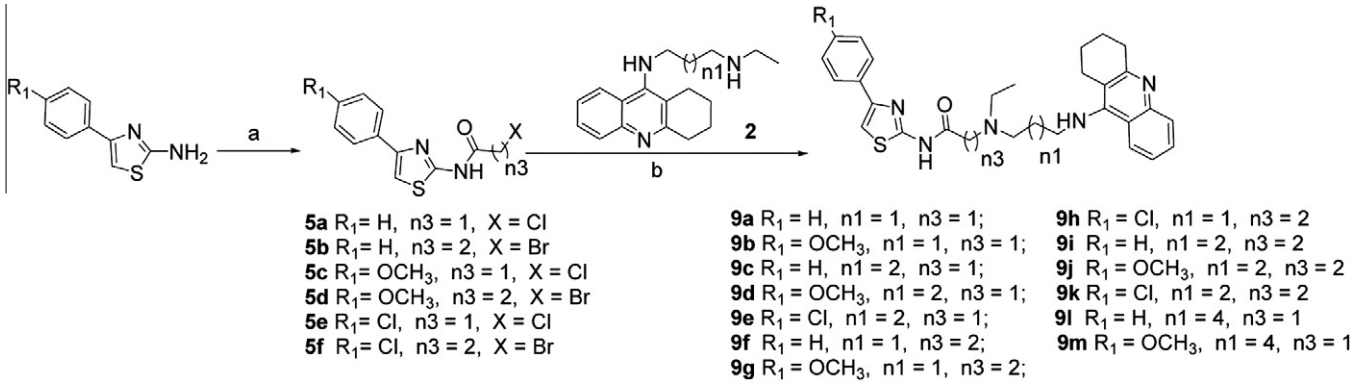

Scheme 2. Synthesis of the second series of phenylthiazole–tacrine hybrids (**9a**–**9m**). Reagents and conditions: (a) chloroacetyl chloride or 3-bromopropionyl chloride, Et_3N, THF/CH_2Cl_2, rt; (b) K_2CO_3/KI, DMF, 70 °C, 2 h.

Table 1
Inhibition of AChE and BuChE (pIC_{50} values) by phenylthiazole–tacrine hybrids and tacrine

Compd	pIC_{50} ± SEM[a]		Selectivity ratio[c]	Compd	pIC_{50} ± SEM[a]		Selectivity ratio[c]
	AChE[b]	BuChE[b]			AChE[b]	BuChE[b]	
7a	6.31 ± 0.01	9.22 ± 0.13	747	**9e**	5.79 ± 0.09	7.11 ± 0.07	21
7b	6.42 ± 0.06	5.75 ± 0.03	0.2	**9f**	6.49 ± 0.04	8.22 ± 0.05	53
7c	7.14 ± 0.01	9.45 ± 0.08	200	**9g**	7.01 ± 0.02	9.32 ± 0.28	150
7d	6.55 ± 0.03	9.26 ± 0.05	514	**9h**	5.92 ± 0.03	8.38 ± 0.09	277
7e	5.87 ± 0.14	7.78 ± 0.04	90	**9i**	6.96 ± 0.06	7.74 ± 0.03	6.3
8	5.90 ± 0.03	6.44 ± 0.02	3.5	**9j**	6.54 ± 0.04	8.18 ± 0.20	42
9a	6.98 ± 0.03	10.35 ± 0.15	2117	**9k**	6.92 ± 0.04	7.34 ± 0.06	2.6
9b	5.86 ± 0.05	6.56 ± 0.03	5	**9l**	7.09 ± 0.09	6.33 ± 0.06	0.2
9c	6.80 ± 0.08	7.83 ± 0.05	11	**9m**	6.80 ± 0.09	6.23 ± 0.01	0.3
9d	5.78 ± 0.05	7.69 ± 0.07	81	Tacrine	7.19 ± 0.03	8.42 ± 0.11	17

[a] Data are the mean values of at least three determinations ± standard error of mean. $pIC_{50} = -\log IC_{50}$.
[b] AChE from electric eel and BuChE from equine serum were used.
[c] Selectivity ratio = (IC_{50} of AChE)/(IC_{50} of BuChE).

with **2** in the presence of K_2CO_3/KI in DMF produced compound **9a**–**9m**.

2.2. Cholinesterase inhibition

Inhibition of AChE and BuChE were determined by the Ellman method, selecting tacrine as reference compound.[23] All phenylthiazole–tacrine hybrids (Table 1) were potent inhibitors of AChE with pIC_{50} ($-\log IC_{50}$) ranging from 5.78 ± 0.05 to 7.14 ± 0.01. In the first series (**7a**–**7e**, and **8**), the length of middle linker affected the AChE inhibitory potency. Compound **7c** displayed the optimal AChE inhibitory potency (AChE pIC_{50} = 7.14 ± 0.01), characteristic of the length of 10 spacer atoms (no counting N atoms). Compared with H at 4′-position of 4-phenyl-2-aminothiazole (**7a**, AChE pIC_{50} = 6.31 ± 0.01), substituting with Cl at 4′-position afforded a slight reduction of AChE inhibition (**7e**, pIC_{50} = 5.87 ± 0.14). When changing 4-phenyl-2-aminothiazole (**7a**) with 4,5,6,7-tetrahydrobenzo[*d*]thiazol-2-amine (**8**), both of the AChE and BuChE pIC_{50} were decreased. In the second series (**9a**–**9m**), the AChE inhibitory potency was sensitive to substitutions at 4′-position of 4-phenyl-2-aminothiazole. Compared with H at 4′-position of 4-phenyl-2-aminothiazole (**9a**, **9c**, **9f**, **9i**, **9l**), substituting with OCH_3 or Cl at 4′-position (**9b**, **9d**, **9e**, **9h**, **9j**, **9k**, **9m**) were less favorable, except **9g** (pIC_{50} = 7.01 ± 0.02) which was slightly potent than **9f** (pIC_{50} = 6.49 ± 0.04). Many reports revealed previously that introduction a diamine side chain to 9-position of tacrine unit or presence of Cl atom at 6-position of tacrine unit could improve the AChE inhibitory activity. However, in this study, phenylthiazole–tacrine hybrids showed a decrease in the inhibitory activity

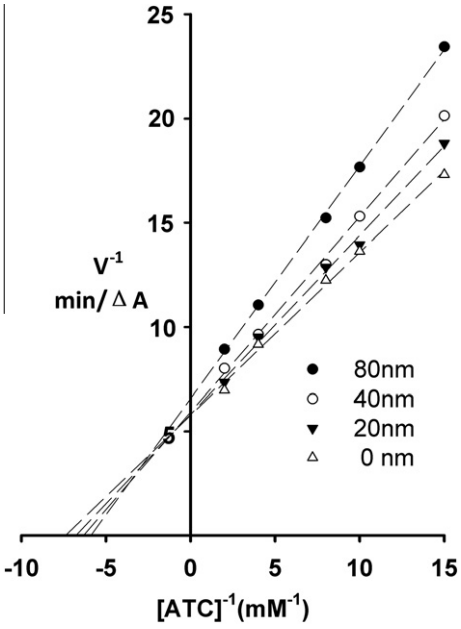

Figure 3. Kinetic study on the mechanism of AChE inhibition by **7c**. Lineweaver–Burk reciprocal plots of AChE initial velocity at increasing substrate concentration (0.067–0.5 mM) in the absence of inhibitor and in the presence of **7c** (20–80 nm) are shown.

Table 2
Inhibition of $A\beta_{1-42}$ self-aggregation by phenylthiazole–tacrine hybrids

Compd	Inhibition of Aβ aggregation % ± SEM[a]	Compd	Inhibition of Aβ aggregation % ± SEM[a]
7a	12.5 ± 3.6	**9e**	63.3 ± 2.6
7b	23.7 ± 1.6	**9f**	51.8 ± 4.1
7c	35.8 ± 5.8	**9g**	59.2 ± 3.6
7d	9.7 ± 3.0	**9h**	57.1 ± 1.3
7e	16.4 ± 3.1	**9i**	54.2 ± 2.8
8	−7.8 ± 4.4	**9j**	58.2 ± 0.8
9a	49.4 ± 3.8	**9k**	39.6 ± 1.2
9b	63.8 ± 4.1	**9l**	69.6 ± 1.1
9c	62.4 ± 1.2	**9m**	72.0 ± 3.4
9d	66.1 ± 2.6	Propidium iodide	57.1 ± 5.7
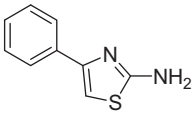	11.2 ± 3.6	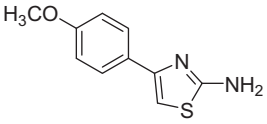	11.6 ± 2.2

[a] Values are expressed as mean ± standard error of the mean from three independent measurements, each performed in duplicate. Inhibition of $A\beta_{1-42}$ self-aggregation with the tested compounds at concentration of 20 μM.

against AChE. The reduced potency of phenylthiazole–tacrine hybrids against AChE might result from an unsuitable linker type or conformation, which wasn't in favor for the nitrogen atom interaction with the mid-gorge recognition site of AChE or the phenylthiazole moiety binding tightly with the peripheral site of AChE.

Considering the therapeutic benefits of BuChE, it was noteworthy that a possible role of BuChE inhibition could contribute to disease modification.[24–26] Phenylthiazole–tacrine hybrids inhibited BuChE with pIC_{50} value ranging from 5.75 ± 0.03 to 10.35 ± 0.15. In some cases, their inhibitory potency (**7a**, **7c**, **7d**, **9a**, **9g**, **9h**) were higher than or comparable to tacrine. Regarding the selectivity profile, phenylthiazole–tacrine hybrids were more potent inhibitors of BuChE than that of AChE, except **7b**, **9l** and **9m**. Particularly, compound **9a** (BuChE pIC_{50} = 10.35 ± 0.15) showed the highest potency and selectivity for BuChE.

2.3. Kinetic characterization of AChE inhibition

The mechanism of AChE inhibition was investigated in vitro by using compound **7c**, the most potent inhibitor of the two series. An analysis of the Lineweaver–Burk reciprocal plots of **7c** against AChE revealed that there were an increasing slope and an increasing intercept with higher inhibitor concentration (Fig. 3). This result indicate that **7c** is characterized by a linear mixed-type of enzyme inhibition and could bind simultaneously with the catalytic and the peripheral sites of AChE. This inhibitory pattern was similar to that of tacrine and other reported tacrine derivatives.[10,12,13]

2.4. Inhibition of self-mediated $A\beta_{1-42}$ aggregation

2.4.1. Thioflavin T fluorescence assay

The ability of phenylthiazole–tacrine hybrids to reduce $A\beta_{1-42}$ self-aggregation was investigated by Thioflavin T (ThT) fluorescence assay, selecting propidium iodide as reference compound. ThT can selectively concentrate in amyloid deposits and display intensive fluorescence emission at 485 nm.[27] As shown in Table 2, the first series (**7a**–**7e** and **8**) were found to be less pronounced to inhibit $A\beta_{1-42}$ self-aggregation at 20 μM, except **7c** (35.8 ± 5.8% at 20 μM). When replacing 4-phenyl-2-aminothiazole (**7a**) with 4,5,6,7-tetrahydrobenzo[*d*]thiazol-2-amine (**8**), **8** turned out to be completely inactive. The second series (**9a**–**9m**) can efficiently block $A\beta_{1-42}$ self-aggregation at 20 μM. Remarkably, nine of synthesized derivatives (**9b**–**9e**, **9g**, **9h, 9j**, **9l**, **9m**) were more potent than the positive control propidium iodide. Among them, **9m** (72.0 ± 3.4% at 20 μM) displayed the highest potency. The second series (**9a**–**9m**) were generally more potent than the first series (**7a**–**7e**, and **8**), indicating that the inhibition efficacy seemed to depend on the type of middle linker. Compared with H at 4′-position of 4-phenyl-2-aminothiazole (**9a**, **9c**, **9f**, **9i**, **9l**), substituting with OCH_3 at 4′-position (**9b**, **9d**, **9g**, **9j**, **9m**) enhanced the potency of $A\beta_{1-42}$ self-aggregation inhibition. 4-Phenyl-2-aminothiazole and 4-(4-methoxyphenyl)thiazol-2-amine, the monomeric parent structure of phenylthiazole–tacrine hybrids, also displayed some extent of $A\beta_{1-42}$ self-aggregation inhibitory potency at 20 μM (11.2 ± 3.6% and 11.6 ± 2.2%). Besides, we further investigated **9l** and **9m** on $A\beta_{1-42}$ aggregation at different concentrations. The concentration-effect curves of **9l** and **9m** in Figure 4 indicated that they could inhibit $A\beta_{1-42}$ self-aggregation in a concentration-dependent manner.

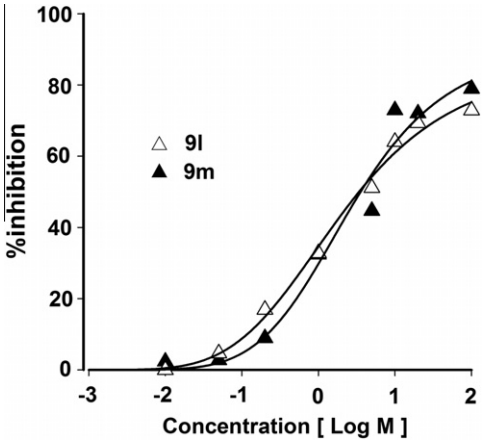

Figure 4. The concentration–effect curves of **9l** (△) and **9m** (▲) determined by the ThT assay.

2.4.2. Atomic force microscopy assay

Due to the nanoscale dimensions and the varied morphology of aggregates, atomic force microscopy (AFM) has emerged as an ideal tool for distinguishing structural features of the aggregate forms.[28] We used AFM as an imaging technique to measure the aggregation process in the absence or presence of **9m**. When 50 μM $A\beta_{1-42}$ was incubated alone in 10% DMSO phosphate buffer (pH 7.4) at 30 °C for 4 days, $A\beta_{1-42}$ converted into robust fibrils and

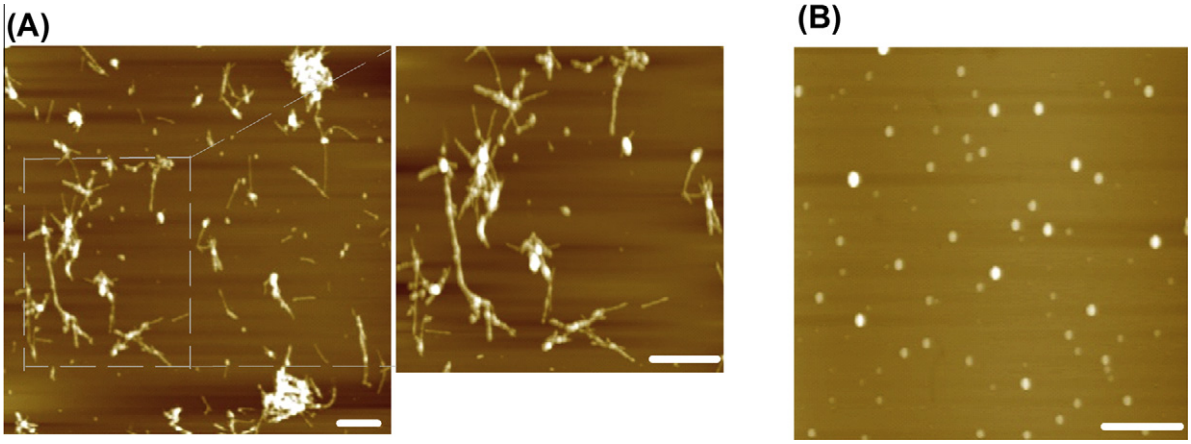

Figure 5. Morphological study of $A\beta_{1-42}$ aggregation by AFM: (A) AFM scan image of 50 μM $A\beta_{1-42}$ incubated alone for 4 days at 30 °C; (B) AFM scan image of 50 μM $A\beta_{1-42}$ incubated with 100 μM **9m** for 4 days at 30 °C. Scale bars are 1 μm.

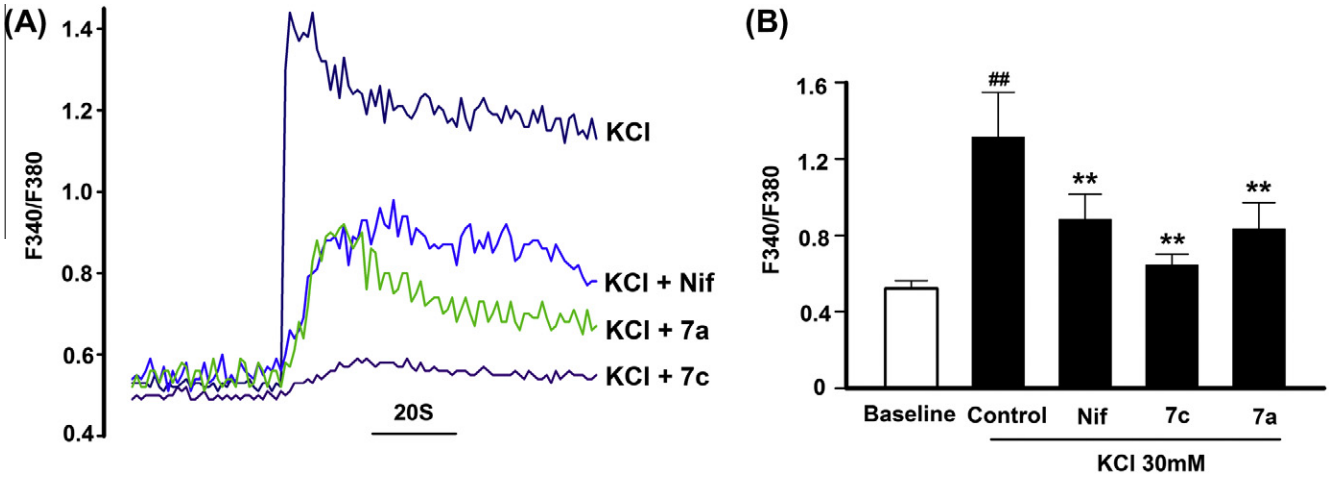

Figure 6. Effect of 1 μM **7a**, **7c**, and nifedipine on the intracellular Ca^{2+} concentration induced by high K^+ (30 mM) in the primary cultured cortical neurons. (A) Representative curves of the F340/F380 ratio in the absence or in the presence of **7a**, **7c**, and nifedipine; (B) statistical analysis of the F340/F380 ratio in the absence (control, $n = 20$) or in the presence of **7a** ($n = 19$), 7c ($n = 21$), or nifedipine ($n = 20$). Experiments were performed from at least three different cell cultures. Data were expressed as mean ± SD. $^{\#\#}p < 0.01$ versus baseline, $^{**}p < 0.01$ versus control group.

large ordered aggregates (Fig. 5A). In contrast, no fibrils but some small aggregates were detected when 100 μM **9m** was added to 50 μM $A\beta_{1-42}$ solution at the same condition (Fig. 5B). Obviously, **9m** effectively prevented the $A\beta_{1-42}$ self-aggregation. The AFM result of **9m** was consistent with the above results of ThT.

2.5. Inhibition of Ca^{2+} overload

Dysregulation of intracellular calcium signaling has been implicated in the pathogenesis of AD. Ca^{2+} overload can cause mitochondrial dysfunction, accumulation of Aβ and tau phosphorylation. Hence, inhibition of Ca^{2+} overload could serve as potential therapeutic approaches for AD prevention and treatment.[29,30] To investigate the potential of Ca^{2+} overload blockade effect, we studied whether **7a**, **7c**, and **9m** displayed any effect on Ca^{2+} overload induced by high K^+ (30 mM) in the primary cultured cortical neurons. The Fluo-2/AM-loaded neurons were incubated in the absence or presence of compounds (1 μM) for 5 min and then stimulated with 30 mM KCl solution. The F340/F380 fluorescence ratio was recorded and used as an indicator of the intracellular Ca^{2+} concentration. 30 mM KCl ($n = 20$) alone induced a significant increase in the ratio of F340/F380 from 0.52 ± 0.04 to 1.31 ± 0.24. In this experiment, we found that **7a** ($n = 19$) and **7c** ($n = 21$) displayed the Ca^{2+} overload blockade effect (Fig. 6). Compound **7c** could decrease the F340/F380 ratio from 1.31 ± 0.24 to 0.64 ± 0.06. **7a** changed the ratio of F340/F380 from 1.31 ± 0.24 to 0.83 ± 0.14. Unfortunately, **9m** ($n > 20$) failed to block the increase of F340/F380 ratio, but caused the ratio of F340/F380 persistent rise. Nifedipine, a calcium channel antagonist, was selected as a positive control. Pretreated with 1 μM Nifedipine ($n = 20$) brought down the F340/F380 ratio from 1.31 ± 0.24 to 0.88 ± 0.13.

3. Conclusion

In this study, a series of phenylthiazole–tacrine hybrids were synthesized and biologically evaluated. Phenylthiazole–tacrine hybrids were potent inhibitors of cholinesterase with pIC_{50} value ranging from 5.78 ± 0.05 to 7.14 ± 0.01 for AChE, and from 5.75 ± 0.03 to 10.35 ± 0.15 for BuChE. They were more potent inhibitors of BuChE than that of AChE, except **7b**, **9l** and **9m**. Compound **9a** (BuChE $pIC_{50} = 10.35 \pm 0.15$) was proved to be the highest potency and selectivity for BuChE. The kinetic characterization

of **7c** was analyzed by using Lineweaver–Burk plots, which revealed that **7c** was a mixed-type inhibitor and could bind simultaneously at the catalytic and the peripheral sites of AChE. Most of phenylthiazole–tacrine hybrids showed a good inhibitory potency on $A\beta_{1-42}$ self-aggregation. Their inhibitory effect depended on the type of middle linker and substitutions at 4′-position of 4-phenyl-2-aminothiazole. Among them, **9m** exhibited the highest inhibitory potency. Additionally, **7a** and **7c** displayed the blockade effect on Ca^{2+} overload in the primary cultured cortical neurons.

4. Experimental

4.1. Chemistry

^1H and ^{13}C NMR spectra were recorded using TMS as the internal standard in $CDCl_3$ or DMSO-d_6 with a Bruker spectrometer at 400 and 100 MHz. The MS spectra were recorded on a Finnigan LCQ Deca XP^{TM} instrument with an ESI mass selective detector. Reactions were monitored by thin layer chromatography and MS spectrometer. Flash column chromatography was performed with silica gel (200–300 mesh) purchased from Qingdao Haiyang Chemical Co. Ltd. The purities of targeted compounds were confirmed by analytical HPLC on a HITACHI L-2000 instrument and a Diamonsil ODS-C18 HPLC column (250 × 4.6 mm, 5 μm) at 340 nm, eluted with a gradient of 90% solvent B (methanol) in solvent A (water) containing 0.2% phosphate buffer (pH 7.23) at a speed of 1 mL/min. The purities of target compounds were determined to be ⩾95% by HPLC unless otherwise indicated.

4.2. Compound 3a–3c and 4 were obtained according to the following general procedure

One molar equivalent of 2-aminothiazole derivatives in 50 mL THF were mixed with 1 molar equiv of succinic anhydride or glutaric anhydride. The reaction solution was refluxed at 65 °C for 7 h, and then evaporated under vacuum to yield crude product. The crude product was dissolved in a cooled aqueous solution of K_2CO_3/KOH, and then filtered to discard the insoluble solid. The combined aqueous phase was acidified by 1 M HCl to pH 1.0 to obtain milk-white deposits. The deposits were then recrystallized from ethyl acetate/ethanol to obtain a pure milk-white powder.

4.2.1. 4-Oxo-4-(4-phenylthiazol-2-ylamino)butanoic acid (3a)

Milk-white powder, yield: 86%. ^1H NMR (DMSO-d_6, 400 MHz, δ ppm): 12.29 (br s, 1H), 12.21 (br s, 1H), 7.88 (d, J = 7.2 Hz, 2H), 7.59 (s, 1H), 7.42 (t, J = 7.2 Hz, 2H), 7.31 (t, J = 7.2 Hz, 1H), 2.69 (t, J = 6.4 Hz, 2H), 2.58 (t, J = 6.4 Hz, 2H). ^{13}C NMR (DMSO-d_6, 100 MHz, δ ppm): 174.0, 171.0, 158.3, 149.2, 134.8, 129.2 (2C), 128.2, 126.1 (2C), 108.3, 30.3, 28.8.

4.2.2. 5-Oxo-5-(4-phenylthiazol-2-ylamino)pentanoic acid (3b)

Milk-white powder, yield: 36%. ^1H NMR (DMSO-d_6, 400 MHz, δ ppm): 12.24 (br s, 1H), 12.12 (br s, 1H), 7.88 (d, J = 7.2 Hz, 2H), 7.58 (s, 1H), 7.41 (t, J = 7.2 Hz, 2H), 7.30 (t, J = 7.2 Hz, 1H), 2.49 (t, J = 7.2 Hz, 2H), 2.28 (t, J = 7.2 Hz, 2H), 1.83 (m, J = 7.2 Hz, 2H). ^{13}C NMR (DMSO-d_6, 100 MHz, δ ppm): 174.5, 171.6, 158.3, 149.2, 134.8, 129.2 (2C), 128.2, 126.1 (2C), 108.3, 34.4, 33.3, 20.4.

4.2.3. 4-(4-(4-Chlorophenyl) thiazol-2-ylamino)-4-oxobutanoic acid (3c)

Milk-white powder, yield: 30%. ^1H NMR (DMSO-d_6/$CDCl_3$, 400 MHz, δ ppm): 7.85 (d, J = 8.8 Hz, 2H), 7.39 (d, J = 8.8 Hz, 2H), 7.36 (s, 1H), 3.33 (br s, 1H), 2.76 (t, J = 6.8 Hz, 2H), 2.63 (t, J = 6.8 Hz, 2H). ^{13}C NMR (DMSO-d_6/$CDCl_3$, 100 MHz, δ ppm): 178.6, 175.5, 163.3, 163.0, 138.3, 137.6, 133.6 (2C), 132.2 (2C), 112.8, 35.1, 33.6.

4.2.4. 4-Oxo-4-(4,5,6,7-tetrahydrobenzo[*d*]thiazol-2-ylamino) butanoic acid (4)

Milk-white powder, yield: 45%. ^1H NMR (DMSO-d_6, 400 MHz, δ ppm): 11.94 (br s, 2H), 2.62–2.58 (m, 4H), 2.54–2.50 (m, 4H), 1.78–1.68 (m, 4H). ^{13}C NMR (DMSO-d_6, 100 MHz, δ ppm): 174.0, 170.3, 155.1, 144.3, 121.4, 30.3, 28.9, 26.5, 23.4, 23.1, 22.7.

4.3. Compound 5a–5f were obtained according to the following general procedure

To a solution of 1 molar equiv of 2-aminothiazole derivatives and 1.5 molar equiv of triethylamine in THF, 1.2 molar equiv of chloroacetyl chloride or 3-bromopropionyl chloride in THF/CH_2Cl_2 was added dropwise at 0 °C. The reaction mixture was stirred at room temperature, and monitored by TLC (petroleum ether/ethyl acetate = 2/1). After reaction complete, the solvent was removed and the residue was purified by flash chromatography (petroleum ether/ethyl acetate = 10/1) to yield the product.

4.3.1. 2-Chloro-*N*-(4-phenylthiazol-2-yl)acetamide (5a)

Off-white powder, yield: 45%. ^1H NMR ($CDCl_3$, 400 MHz, δ ppm): 10.6 (br s, 1H), 7.83 (d, J = 7.2 Hz, 2H), 7.45 (t, J = 7.2 Hz, 2H), 7.37 (t, J = 7.2 Hz, 1H), 7.02 (s, 1H), 4.06 (s, 2H). ^{13}C NMR ($CDCl_3$, 100 MHz, δ ppm): 164.3, 157.4, 150.2, 134.1, 128.9 (2C), 128.4, 126.2 (2C), 108.5, 41.9.

4.3.2. 3-Bromo-*N*-(4-phenylthiazol-2-yl)propanamide (5b)

Off-white powder, yield: 52%. ^1H NMR ($CDCl_3$, 400 MHz, δ ppm): 11.0 (br s, 1H), 7.74 (d, J = 7.2 Hz, 2H), 7.45 (t, J = 7.2 Hz, 2H), 7.38 (t, J = 7.2 Hz, 1H), 7.13 (s, 1H), 3.58 (t, J = 6.8 Hz, 2H), 2.82 (t, J = 6.8 Hz, 2H). ^{13}C NMR ($CDCl_3$, 100 MHz, δ ppm): 168.3, 159.8, 149.4, 133.7, 129.0(2C), 128.8, 126.4 (2C), 108.2, 38.8, 25.5.

4.3.3. 2-Chloro-*N*-(4-(4-methoxyphenyl)thiazol-2-yl)acetamide (5c)

Off-white powder, yield: 35%. ^1H NMR ($CDCl_3$, 400 MHz, δ ppm): 10.3 (br s, 1H), 7.76 (d, J = 8.8 Hz, 2H), 7.07 (s, 1H), 6.96 (d, J = 8.8 Hz, 2H), 4.13 (s, 2H), 3.86 (s, 3H). ^{13}C NMR ($CDCl_3$, 100 MHz, δ ppm): 164.1, 159.8, 157.1, 150.0, 127.5 (2C), 126.9, 114.2 (2C), 106.7, 55.4, 41.9.

4.3.4. 3-Bromo-*N*-(4-(4-methoxyphenyl)thiazol-2-yl)propanamide (5d)

Off-white powder, yield: 26%. ^1H NMR ($CDCl_3$, 400 MHz, δ ppm): 11.90 (br s, 1H), 7.74 (d, J = 8.8 Hz, 2H), 7.07 (s, 1H), 6.96 (d, J = 8.8 Hz, 2H), 3.84 (s, 3H), 3.4 (t, J = 7.6 Hz, 2H), 2.46 (t, J = 7.6 Hz, 2H).

4.3.5. 2-Chloro-*N*-(4-(4-chlorophenyl)thiazol-2-yl)acetamide (5e)

Off-white powder, yield: 52%. ^1H NMR ($CDCl_3$, 400 MHz, δ ppm): 9.73 (br s, 1H), 7.78 (d, J = 8.4 Hz, 2H), 7.35 (d, J = 8.4 Hz, 2H), 7.20 (s, 1H), 4.31 (s, 2H).

4.3.6. 3-Bromo-*N*-(4-(4-chlorophenyl)thiazol-2-yl)propanamide (5f)

Off-white powder, yield: 21%. ^1H NMR ($CDCl_3$, 400 MHz, δ ppm): 11.30 (br s, 1H), 7.73 (d, J = 8.4 Hz, 2H), 7.41(d, J = 8.4 Hz, 2H), 7.17 (s, 1H), 3.53 (t, J = 6.8 Hz, 2H), 2.70 (t, J = 6.8 Hz, 2H). ^{13}C NMR ($CDCl_3$, 100 MHz, δ ppm): 168.1, 159.1, 148.5, 134.3, 132.4, 129.2 (2C), 127.5 (2C), 108.6, 38.9, 25.3.

4.4. Compound 7a–7e, 8 were obtained according to the following general procedure

To a stirred solution of 1.2 molar equiv of compound **3** or **4** in DMF/CH_2Cl_2 at 25 °C was added 1.5 molar equiv of 1-ethyl-3-(3-diethylaminopropyl)carbodiimide (EDC·HCl) and 1.5 molar equiv of hydroxybenzotriazole (HOBt). The resulting mixture was stirred at room temperature for 30 min before a solution of 1.0 molar equiv of **1** in CH_2Cl_2 was added. The resulting mixture was stirred at 25 °C for 12 h before it was quenched with brine and diluted with CH_2Cl_2. The combined organic phase was dried over Na_2SO_4 and filtered. After removal of the solvent under vacuum, the residue was purified by flash column chromatography with petroleum ether/ethyl acetate containing 0.5% triethylamine to yield the products.

4.4.1. N^1-(4-Phenylthiazol-2-yl)-N^4-(4-(1,2,3,4-tetrahydroacridin-9-ylamino)butyl)succinamide (7a)

White powder, yield: 57%. Purity: 97.4%, t_R = 6.19 min. ^{1}H NMR (DMSO-d_6, 400 MHz, δ ppm): 7.94 (d, J = 9.6 Hz, 1H), 7.91 (d, J = 9.6 Hz, 1H), 7.80 (d, J = 7.2 Hz, 2H), 7.54 (m, 1H), 7.37 (t, J = 7.2 Hz, 2H), 7.31 (m, 2H), 7.07 (s, 1H), 5.93 (br s, 1H), 4.04 (br s, 1H), 3.47 (t, J = 6.8 Hz, 2H), 3.33 (m ,2H), 3.06 (m, 2H), 2.75 (m, 2H), 2.67 (m, 2H), 2.58 (m, 2H), 1.89 (m, 4H), 1.64 (m, 4H). ^{13}C NMR (DMSO-d_6, 100 MHz, δ ppm): 171.9, 170.3, 158.4, 157.6, 150.5, 149.9, 147.2, 134.4, 128.6 (2C), 128.5, 128.4, 128.0, 126.1 (2C), 123.8, 122.7, 120.3, 116.3, 107.5, 48.8, 39.4, 33.9, 31.5, 31.1, 28.8, 27.1, 24.8, 23.0, 22.7. ESI-MS [M+H]$^+$ (m/z): 528.4. $C_{30}H_{33}N_5O_2S$ [527.24].

4.4.2. N^1-(4-Phenylthiazol-2-yl)-N^5-(3-(1,2,3,4-tetrahydroacridin-9-ylamino)propyl)glutaramide (7b)

Colorless powder, yield: 39%. Purity: 99.1%, t_R = 6.34 min. ^{1}H NMR (DMSO-d_6, 400 MHz, δ ppm): 12.21 (br s, 1H), 8.10 (d, J = 8.0 Hz, 1H), 7.88 (m, 3H), 7.68 (d, J = 8.0 Hz, 1H), 7.59 (s, 1H), 7.49 (t, J = 7.2 Hz, 1H), 7.42 (t, J = 7.2 Hz, 2H), 7.32 (t, J = 7.2 Hz, 1H), 7.31 (t, J = 6.8 Hz, 1H), 5.52 (t, J = 6.8 Hz, 1H), 3.87 (m, 2H), 3.09 (m, 2H), 2.88 (t, J = 6.0 Hz, 2H), 2.70 (t, J = 6.0 Hz, 2H), 2.44 (t, J = 7.2 Hz, 2H), 2.11 (t, J = 7.2 Hz, 2H), 1.82 (m, 6H), 1.64 (m, 2H) ^{13}C NMR (DMSO-d_6, 100 MHz, δ ppm): 172.2, 171.6, 158.4, 158.3, 150.6, 149.2, 147.4, 134.8, 129.2, 128.8(2C), 128.2, 126.1(2C), 123.8, 123.3, 120.8, 116.5, 108.3, 45.6, 36.4, 34.9, 34.7, 34.0, 31.2, 25.6, 23.2, 22.9, 21.3. ESI-MS [M+H]$^+$ (m/z): 528.4. $C_{30}H_{33}N_5O_2S$ [527.24]..

4.4.3. N^1-(4-Phenylthiazol-2-yl)-N^4-(6-(1,2,3,4-tetrahydroacridin-9-ylamino)hexyl)succinamide (7c)

Off-white powder, yield: 17%. Purity: 94.2%, t_R = 8.35 min. ^{1}H NMR (DMSO-d_6, 400 MHz, δ ppm): 7.96 (d, J = 8.4 Hz, 1H), 7.94 (d, J = 8.4 Hz, 1H), 7.80 (d, J = 7.2 Hz, 2H), 7.56 (td, J = 7.6 and 0.8 Hz, 1H), 7.38 (t, J = 7.2 Hz, 2H), 7.36 (m, 1H), 7.30 (m, 1H), 7.08 (s, 1H), 5.82 (m, 1H), 4.13 (br s, 1H), 3.47 (t, J = 7.2 Hz, 2H), 3.28 (q, J = 7.2 Hz, 2H), 3.08 (m, 2H), 2.79 (m, 2H), 2.67 (m, 2H), 2.61 (m, 2H), 1.91 (m, 4H), 1.62 (m, J = 7.2 Hz, 2H), 1.50 (m, 2H), 1.35 (m, 4H). ^{13}C NMR (DMSO-d_6, 100 MHz, δ ppm): 171.8, 170.4, 158.4, 157.7, 150.7, 149.9, 147.4, 134.4, 128.6 (2C), 128.6, 128.3, 127.9, 126.1 (2C), 123.6, 122.8, 120.2, 115.9, 107.4, 49.2, 39.6, 33.9, 31.6, 31.1, 29.5, 26.5 (2C), 24.8, 23.0, 22.7. ESI-MS [M+H]$^+$ (m/z): 556.4. $C_{32}H_{37}N_5O_2S$ [555.27].

4.4.4. N^1-(4-Phenylthiazol-2-yl)-N^5-(4-(1,2,3,4-tetrahydroacridin-9-ylamino)butyl)glutaramide (7d)

Off-white powder, yield: 49%. Purity: 99.7%, t_R = 6.55 min. ^{1}H NMR (DMSO-d_6, 400 MHz, δ ppm): 12.22 (br s, 1H), 8.10 (d, J = 8.0 Hz, 1H), 7.87 (d, J = 8.0 Hz, 2H), 7.78 (t, J = 5.6 Hz, 1H), 7.68 (d, J = 8.0 Hz, 1H), 7.58 (s, 1H), 7.50 (td, J = 7.6 and 0.8 Hz, 1H), 7.41 (t, J = 7.6 Hz, 2H), 7.32 (td, J = 6.8 and 0.8 Hz, 1H), 7.30 (m, 1H), 5.42 (t, J = 5.6 Hz, 1H), 3.30 (q, J = 6.8 Hz, 2H), 3.01 (m, 2H), 2.88 (m, 2H), 2.69 (m, 2H), 2.44 (t, J = 7.2 Hz, 2H), 2.08 (t, J = 7.6 Hz, 2H), 1.80 (m, 6H), 1.53 (m, J = 7.2 Hz, 2H), 1.41 (m, J = 7.2 Hz, 2H). ^{13}C NMR (DMSO-d_6, 100 MHz, δ ppm): 172.6, 171.1, 158.5, 158.3, 150.7, 149.7, 147.0, 134.4, 128.7 (2C), 128.5, 128.2, 128.1, 126.1 (2C), 123.8, 122.8, 120.2, 116.2, 107.6, 48.8, 39.1, 35.1, 34.8, 33.7, 28.9, 27.1, 24.8, 22.9, 22.6, 21.2. ESI-MS [M+H]$^+$ (m/z): 542.3. $C_{31}H_{35}N_5O_2S$ [541.25].

4.4.5. N^1-(4-(4-Chlorophenyl)thiazol-2-yl)-N^4-(4-(1,2,3,4-tetrahydroacridin-9-ylamino)butyl)succinamide (7e)

Off-white powder, yield: 18%. Purity: 95.7%, t_R = 8.31 min. ^{1}H NMR (DMSO-d_6, 400 MHz, δ ppm): 12.24 (br s, 1H), 8.09 (d, J = 8.4 Hz, 1H), 7.89 (d, J = 8.4 Hz, 2H), 7.86 (t, J = 5.6 Hz, 1H), 7.69 (d, J = 8.8 Hz, 1H), 7.63 (s, 1H), 7.50 (td, J = 7.6 and 0.8 Hz, 1H), 7.47 (d, J = 8.4 Hz, 2H), 7.32 (td, J = 7.4 and 1.2 Hz, 1H), 5.36 (t, J = 6.0 Hz, 1H), 3.37 (q, J = 6.8 Hz, 2H), 3.1 (m, 2H), 2.88 (t, J = 6.0 Hz, 2H), 2.70–2.63 (m, 4H), 2.40 (t, J = 6.8 Hz, 2H), 1.81–1.74 (m, 4H), 1.57–1.50 (m, 2H), 1.44–1.35 (m, 2H). ^{13}C NMR (DMSO-d_6, 100 MHz, δ ppm): 171.4, 171.1, 158.6, 158.3, 150.7, 147.9, 147.3, 133.7, 132.6, 129.2(2C), 128.7, 128.3, 127.8(2C), 123.7, 123.5, 120.7, 116.3, 109.0, 48.1, 38.7, 34.0, 30.8, 30.1, 28.5, 27.0, 25.5, 23.2, 22.9. ESI-MS [M+H]$^+$ (m/z): 562.2. $C_{30}H_{32}ClN_5O_2S$ [561.20].

4.4.6. N^1-(4-(1,2,3,4-Tetrahydroacridin-9-ylamino)butyl)-N^4-(4,5,6,7-tetrahydrobenzo[*d*]thiazol-2-yl)succinamide (8)

Off-white powder, yield: 44%. Purity: 98.9%, t_R = 6.17 min. ^{1}H NMR (DMSO-d_6, 400 MHz, δ ppm): 11.81 (br s, 1H), 8.08 (d, J = 8.0 Hz, 1H), 7.83 (t, J = 5.6 Hz, 1H), 7.68 (d, J = 8.8 Hz, 1H), 7.50 (td, J = 7.8 and 1.2 Hz, 1H), 7.32 (td, J = 7.8 and 1.2 Hz, 1H), 5.33 (t, J = 6.4 Hz, 1H), 3.36 (q, J = 6.8 Hz, 2H), 3.00 (q, J = 6.4 Hz, 2H), 2.89 (t, J = 6.4 Hz, 2H), 2.69 (t, J = 6.0 Hz, 2H), 2.59–2.55 (m, 4H), 2.52 (m, 2H), 2.36 (t, J = 6.8 Hz, 2H), 1.82–1.77 (m, 4H), 1.76–1.73 (m, 4H), 1.57–1.49 (m, J = 7.2 Hz, 2H), 1.43–1.35(m, J = 7.2 Hz, 2H). ^{13}C NMR (DMSO-d_6, 100 MHz, δ ppm): 171.2, 170.6, 158.4, 155.2, 150.7, 147.4, 144.3, 128.8, 128.3, 123.7, 123.5, 121.3, 120.7, 116.3, 48.1, 38.7, 34.0, 30.8, 30.2, 28.5, 27.0, 26.4, 25.5, 23.4, 23.2, 23.1, 22.9, 22.7. ESI-MS [M+H]$^+$ (m/z): 506.3. $C_{28}H_{35}N_5O_2S$ [505.25].

4.5. Compound 9a–9m were obtained according to the following general procedure

To a solution of 1 molar equiv of **2** in 10 mL DMF was added 1 molar equiv of compound **5** or **6** in presence of K_2CO_3/KI. The reaction mixture was stirred at 70 °C for 2 h, and then diluted with CH_2Cl_2, washed with brine to remove DMF. The combined organic phase was dried over Na_2SO_4 and filtered. After removal of the solvent under vacuum, the residue was purified by flash column chromatography with petroleum ether/ethyl acetate 0.5% triethylamine to yield the products.

4.5.1. 2-(Ethyl(3-(1,2,3,4-tetrahydroacridin-9-ylamino)propyl)amino)-*N*-(4-phenylthiazol-2-yl)acetamide (9a)

Pale yellow oil, yield: 82%. Purity: 99.1%, t_R = 10.50 min. ^{1}H NMR ($CDCl_3$, 400 MHz, δ ppm): 10.54 (br s, 1H), 7.96 (d, J = 8.8 Hz, 1H), 7.94 (d, J = 8.8 Hz, 1H), 7.72 (d, J = 7.6 Hz, 2H), 7.54 (t, J = 7.6 Hz, 1H), 7.39 (m, 2H), 7.32 (m, 2H), 7.15 (s, 1H), 3.57 (t, J = 6.8 Hz, 2H), 3.34 (s, 2H), 3.05 (t, J = 6.8 Hz, 2H), 2.72 (m, 6H), 1.91 (t, J = 7.2 Hz, 2H), 1.86 (m, 4H), 1.13 (t, J = 7.2 Hz, 3H). ^{13}C NMR ($CDCl_3$, 100 MHz, δ ppm): 169.9, 158.4, 156.9, 150.6, 150.2, 147.1, 134.3, 128.7 (3C), 128.5, 128.0, 126.0 (2C), 124.1, 122.5, 120.3, 116.7, 107.7, 57.5, 52.8, 49.3, 47.4, 33.7, 29.3, 24.9, 22.9, 22.6, 11.9. ESI-MS [M+H]$^+$ (m/z): 500.3. $C_{29}H_{33}N_5OS$ [499.24].

4.5.2. 2-(Ethyl(3-(1,2,3,4-tetrahydroacridin-9-ylamino)propyl) amino)-*N*-(4-(4-methoxyphenyl)thiazol-2-yl)acetamide (9b)

Pale yellow oil, yield: 61%. Purity: 96.6%, t_R = 10.58 min. ^{1}H NMR ($CDCl_3$, 400 MHz, δ ppm): 10.53 (br s, 1H), 7.95 (d, J = 8.0 Hz, 1H), 7.92 (d, J = 8.0 Hz, 1H), 7.65 (d, J = 8.8 Hz, 2H), 7.54 (t, J = 8.0 Hz, 1H), 7.34 (t, J = 8.0 Hz, 1H), 7.01 (s, 1H), 7.65 (d, J = 8.8 Hz, 2H), 4.00 (br s, 1H), 3.85 (s, 3H), 3.55 (t, J = 7.2 Hz, 2H), 3.33 (s, 2H), 3.06 (t, J = 6.0 Hz, 2H), 2.71 (m, 6H), 1.88 (m, 6H), 1.12 (t, J = 7.2 Hz, 3H). ^{13}C NMR ($CDCl_3$, 400 MHz, δ ppm): 169.8, 159.5, 158.7, 156.8, 150.4, 150.0, 147.4, 128.9, 128.4, 127.3 (2C), 127.2, 124.0, 122.5, 120.5, 116.9, 114.1 (2C), 106.0, 57.6, 55.3, 52.8, 49.4, 47.5, 34.0, 29.3, 24.9, 22.9, 22.7, 11.8. ESI-MS $[M+H]^+$ (m/z): 530.3. $C_{30}H_{35}N_5O_2S$ [529.25].

4.5.3. 2-(Ethyl(4-(1,2,3,4-tetrahydroacridin-9-ylamino)butyl) amino)-*N*-(4-phenylthiazol-2-yl)acetamide (9c)

Pale yellow oil, yield: 63%. Purity: 96.1%, t_R = 11.58 min. ^{1}H NMR ($CDCl_3$, 400 MHz, δ ppm): 10.50 (br s, 1H), 7.92 (d, J = 7.6 Hz, 1H), 7.91 (d, J = 7.6 Hz, 1H), 7.83 (d, J = 7.2 Hz, 2H), 7.54 (m, 1H), 7.40 (t, J = 7.6 Hz, 2H), 7.33 (m, 2H), 7.16 (s, 1H),3.50 (t, J = 7.2 Hz,2H), 3.29 (s, 2H), 2.69 (m, 4H), 2.61 (t, J = 7.2 Hz, 2H), 1.88 (m, 4H), 1.73 (m, 2H), 1.62 (m, 2H), 1.11 (t, J = 7.2 Hz, 3H). ^{13}C NMR ($CDCl_3$, 100 MHz, δ ppm): 170.1, 158.5, 157.0, 150.5, 150.2, 147.4, 134.4, 128.7 (3C), 128.3, 128.0, 126.1 (2C), 123.8, 122.6, 120.4, 116.4, 107.8, 57.4, 54.9, 49.3, 49.1, 40.0, 29.6, 24.8, 24.7, 23.0, 22.7, 11.9. ESI-MS $[M+H]^+$ (m/z): 514.3. $C_{30}H_{35}N_5OS$ [513.26].

4.5.4. 2-(Ethyl(4-(1,2,3,4-tetrahydroacridin-9-ylamino)butyl) amino)-*N*-(4-(4-methoxyphenyl)thiazol-2-yl)acetamide (9d)

Pale yellow oil, yield: 43%. Purity: 98.1%, t_R = 11.50 min. ^{1}H NMR ($CDCl_3$, 400 MHz, δ ppm): 10.48 (br s, 1H), 7.95 (d, J = 7.6 Hz, 1H), 7.93 (d, J = 7.6 Hz, 1H), 7.75 (d, J = 8.8 Hz, 2H), 7.55 (m ,1H), 7.34 (m, 1H), 7.02 (s, 1H), 6.92 (d, 2H), 3.84 (s, 3H), 3.52 (t, J = 7.2 Hz, 2H), 3.29 (s, 2H), 3.07 (t, J = 6.0 Hz, 2H), 2.68 (m, 4H), 2.61 (t, J = 7.2 Hz, 2H), 1.88 (m, 4H), 1.74 (m, 2H), 1.62 (m, 2H), 1.11 (t, J = 7.2 Hz, 3H). ^{13}C NMR ($CDCl_3$, 100 MHz, δ ppm): 170.0, 159.5, 158.2, 156.9, 150.7, 149.9, 128.6, 128.4, 128.3, 127.4 (2C), 127.7, 123.9, 122.7, 120.1, 116.1, 114.1 (2C), 106.1, 57.4, 55.3, 54.9, 49.3, 49.1, 33.7, 29.6, 24.8, 24.7, 22.9, 22.6, 11.9. ESI-MS $[M+H]^+$ (m/z): 544.3. $C_{31}H_{37}N_5O_2S$ [543.27].

4.5.5. *N*-(4-(4-Chlorophenyl)thiazol-2-yl)-2-(ethyl(4-(1,2,3,4-tetrahydroacridin-9-ylamino)butyl)amino)acetamide (9e)

Light brown oil, yield: 94%. Purity: 98.3%, t_R = 14.81 min. ^{1}H NMR ($CDCl_3$, 400 MHz, δ ppm): 10.47 (br s, 1H), 7.90 (d, J = 7.6 Hz, 1H), 7.88 (d, J = 7.6 Hz, 1H), 7.74 (d, J = 8.4 Hz, 2H), 7.52 (m, 2H), 7.33 (d, J = 8.4 Hz, 2H), 7.29 (m, 1H), 7.11 (s, 1H), 3.47 (t, J = 7.2 Hz, 2H), 3.27 (s, 2H), 3.03 (t, J = 6.0 Hz, 2H), 2.66 (m, 4H), 2.59 (m, 2H), 1.85 (m, 4H), 1.69 (m, 2H), 1.59 (m, 2H), 1.08 (t, J = 7.2 Hz, 3H). ^{13}C NMR ($CDCl_3$, 100 MHz, δ ppm): 170.1, 158.3, 157.2, 150.5, 148.9, 147.2, 133.7, 132.9, 128.8 (2C), 128.6, 128.4, 127.3 (2C), 123.8, 122.6, 120.2, 116.3, 108.1, 57.4, 54.9, 49.3, 49.1, 33.8, 29.5, 24.8, 24.7, 22.9, 22.7, 11.9. ESI-MS $[M+H]^+$ (m/z): 548.3. $C_{30}H_{34}ClN_5OS$ [547.22].

4.5.6. 3-(Ethyl(3-(1,2,3,4-tetrahydroacridin-9-ylamino)propyl) amino)-*N*-(4-phenylthiazol-2-yl)propanamide (9f)

Pale yellow oil, yield: 45%. Purity: 95.7%, t_R = 8.82 min. ^{1}H NMR ($CDCl_3$, 400 MHz, δ ppm): 12.73 (br s, 1H), 7.91 (d, J = 8.4 Hz, 1H), 7.89 (d, J = 8.4 Hz, 1H), 7.81 (d, J = 7.6 Hz, 2H), 7.51 (t, J = 7.6 Hz, 1H), 7.31 (t, J = 7.6 Hz, 2H), 7.25 (m, 2H), 7.13 (s, 1H), 4.33 (br s, 1H), 3.71 (t, J = 6.8 Hz, 2H), 2.99 (t, J = 6.4 Hz, 2H), 2.82 (t, J = 6.0 Hz, 2H), 2.72 (q, J = 7.2 Hz, 2H), 2.65 (t, J = 6.8 Hz, 2H), 2.58 (m, 4H), 1.95 (t, J = 6.8 Hz, 2H), 1.79 (m, 4H), 1.15 (t, J = 7.2 Hz, 3H). ^{13}C NMR ($CDCl_3$, 100 MHz, δ ppm): 170.2, 158.5, 157.5, 150.2, 150.0, 147.3, 134.4, 128.7, 128.6(2C), 128.2, 127.8, 126.0 (2C), 123.7, 122.4, 120.3, 116.3, 107.4, 50.5, 48.9, 46.9, 46.2, 33.9, 31.8, 28.8, 24.9, 22.9, 22.7, 10.6. ESI-MS $[M+H]^+$ (m/z): 514.3. $C_{30}H_{35}N_5OS$ [513.26].

4.5.7. 3-(Ethyl(3-(1,2,3,4-tetrahydroacridin-9-ylamino) propyl)amino)-*N*-(4-(4-methoxyphenyl)thiazol-2-yl) propanamide (9g)

Pale yellow foam, yield: 49%. Purity: 98.7%, t_R = 9.69 min. ^{1}H NMR ($CDCl_3$, 400 MHz, δ ppm) : 12.71 (br s, 1H), 7.92 (d, J = 8.4 Hz, 2H), 7.72 (d, J = 8.8 Hz, 2H), 7.52 (m, 1H), 7.27 (m, 1H), 7.25 (m, 1H), 6.99 (s, 1H), 6.82 (d, J = 8.8 Hz, 2H), 4.48 (br s, 1H), 3.80 (s, 3H), 3.75 (m, 2H), 3.01 (t, J = 6.0 Hz, 2H), 2.83 (t, J = 6.0 Hz, 2H), 2.73 (q, J = 7.2 Hz, 2H), 2.66 (t, J = 6.4 Hz, 2H), 2.58 (m, 4H), 1.96 (t, J = 7.2 Hz, 2H), 1.79 (m, 4H), 1.16 (t, J = 7.2 Hz, 3H). ^{13}C NMR ($CDCl_3$, 100 MHz, δ ppm): 170.2, 159.4, 158.5, 157.5, 150.2, 149.8, 147.3, 128.7, 128.3, 127.4, 127.2(2C), 123.7, 122.5, 120.3, 116.3, 114.0 (2C), 105.6, 55.3, 50.6, 48.9, 47.0, 46.2, 33.9, 31.9, 28.8, 24.9, 22.9, 22.7, 10.6. ESI-MS $[M+H]^+$ (m/z): 544.3. $C_{31}H_{37}N_5O_2S$ [543.27].

4.5.8. *N*-(4-(4-Chlorophenyl)thiazol-2-yl)-3-(ethyl(3-(1,2,3,4-tetrahydroacridin-9-yl amino)propyl)amino)propanamide (9h)

Pale yellow foam, yield: 37%. Purity: 99.8%, t_R = 12.66 min. ^{1}H NMR ($CDCl_3$, 400 MHz, δ ppm): 12.77 (br s, 1H), 7.92 (m, 2H), 7.72 (d, J = 8.8 Hz, 2H), 7.51 (t, J = 7.2 Hz, 1H), 7.27 (m, 2H), 7.25 (m, 2H), 7.11 (s, 1H), 4.41 (br s, 1H), 3.73 (m, 2H), 3.02 (t, J = 6.0 Hz, 2H), 2.84 (t, J = 6.0 Hz, 2H), 2.75 (q, J = 7.2 Hz, 2H), 2.68 (t, J = 6.8 Hz, 2H), 2.59 (m, 4H), 1.96 (m, 2H), 1.81 (m, 4H), 1.17 (t, J = 7.2 Hz, 3H). ^{13}C NMR ($CDCl_3$, 100 MHz, δ ppm): 170.2, 158.6, 157.6, 150.1, 148.8, 147.4, 133.5, 132.9, 128.8, 128.7 (2C), 128.3, 127.2 (2C), 123.8, 122.3, 120.3, 116.4, 107.7, 50.5, 48.9, 47.0, 46.2, 34.0, 31.9, 28.8, 24.9, 22.9, 22.7, 10.6. ESI-MS $[M+H]^+$ (m/z): 548.2. $C_{30}H_{34}ClN_5OS$ [547.22].

4.5.9. 3-(Ethyl(4-(1,2,3,4-tetrahydroacridin-9-ylamino)butyl) amino)-*N*-(4-phenylthiazol-2-yl)propanamide (9i)

Pale yellow oil, yield: 96%. Purity: 99.1%, t_R = 9.68 min. ^{1}H NMR ($CDCl_3$, 400 MHz, δ ppm) : 12.95 (br s, 1H), 7.85 (d, J = 8.0 Hz, 1H), 7.84 (d, J = 8.0 Hz, 1H), 7.79 (d, J = 8.0 Hz, 2H), 7.47 (t, J = 8.0 Hz, 2H), 7.22 (m, 4H), 7.07 (s, 1H), 3.47 (t, J = 7.2 Hz, 2H), 2.96 (t, J = 6.4 Hz, 2H), 2.75 (t, J = 6.0 Hz, 2H), 2.64 (q, J = 7.2 Hz, 2H), 2.53 (m, 4H), 2.42 (t, J = 6.4 Hz, 2H), 1.78 (m, 4H), 1.67 (m, 4H), 1.11 (t, J = 7.2 Hz, 3H). ^{13}C NMR ($CDCl_3$, 100 MHz, δ ppm): 170.4, 158.2, 157.5, 150.7, 149.8, 147.1, 134.5, 128.5 (2C), 128.4, 128.3, 127.8, 125.8 (2C), 123.6, 122.8, 120.1, 116.0, 107.2, 52.3, 49.2, 48.9, 46.2, 33.8, 31.8, 29.6, 24.5, 24.3, 22.9, 22.6, 10.8. ESI-MS $[M+H]^+$ (m/z): 528.3. $C_{31}H_{37}N_5OS$ [527.27].

4.5.10. 3-(Ethyl(4-(1,2,3,4-tetrahydroacridin-9-ylamino)butyl) amino)-*N*-(4-(4-methoxyphenyl)thiazol-2-yl)propanamide (9j)

Pale yellow foam, yield: 85%. Purity: 98.7%, t_R = 9.54 min. ^{1}H NMR ($CDCl_3$, 400 MHz, δ ppm): 12.96 (br s, 1H), 7.87 (d, J = 8.4 Hz, 2H), 7.75 (d, J = 8.4 Hz, 2H), 7.51 (m, 1H), 7.27 (m, 1H), 6.98 (s, 1H), 6.79 (d, J = 8.4 Hz, 2H), 3.92 (br s, 1H), 3.74 (s, 3H), 3.51 (t, J = 6.8 Hz, 2H), 2.99 (t, J = 6.4 Hz, 2H), 2.80 (t, J = 6.4 Hz, 2H), 2.71 (q, J = 7.2 Hz, 2H), 2.59 (m, 4H), 2.46 (t, J = 6.4 Hz, 2H), 1.83 (m, 4H), 1.73 (m, 4H), 1.17 (t, J = 7.2 Hz, 3H). ^{13}C NMR ($CDCl_3$, 100 MHz, δ ppm): 170.3, 159.3, 158.4, 157.4, 150.6, 149.7, 147.4, 128.7, 128.2, 127.5, 127.2 (2C), 123.6, 122.7, 120.3, 116.3, 113.9 (2C), 105.5, 55.2, 52.4, 49.3, 48.9, 46.1, 33.9, 31.8, 29.7, 24.5, 24.3, 22.9, 22.7, 10.7. ESI-MS $[M+H]^+$ (m/z): 558.3. $C_{32}H_{39}N_5O_2S$ [557.28].

4.5.11. N-(4-(4-Chlorophenyl)thiazol-2-yl)-3-(ethyl(4-(1,2,3,4-tetrahydroacridin-9-ylamino)butyl)amino)propanamide (9k)

Pale yellow oil, yield: 60%. Purity: 97.6%, t_R = 13.74 min. ^{1}H NMR ($CDCl_3$, 400 MHz, δ ppm): 13.04 (br s, 1H), 7.89 (d, J = 8.0 Hz, 1H),

7.84 (d, J = 8.0 Hz, 1H), 7.55 (d, J = 8.0 Hz, 2H), 7.52 (d, J = 8.0 Hz, 1H), 7.27 (m, 2H), 7.24 (m, 1H), 7.10 (s, 1H), 3.91 (br s, 1H), 3.51 (t, J = 6.8 Hz, 2H), 3.01 (t, J = 6.4 Hz, 2H), 2.81 (t, J = 6.4 Hz, 2H), 2.72 (q, J = 7.2 Hz, 2H), 2.60 (m, 4H), 2.48 (t, J = 6.4 Hz, 2H), 1.84 (m, 4H), 1.75 (m, 4H), 1.18 (t, J = 7.2 Hz, 3H). ^{13}C NMR ($CDCl_3$, 100 MHz, δ ppm):170.4, 158.3, 157.7, 150.6, 148.8, 147.2, 133.5, 133.0, 128.7 (2C), 128.6, 128.3, 127.1 (2C), 123.7, 122.6, 120.2, 116.2, 107.6, 52.4, 49.3, 48.9, 46.2, 33.9, 31.7, 29.7, 24.6, 24.3, 22.9, 22.7, 10.8. ESI-MS $[M+H]^+$ (m/z): 562.3. $C_{31}H_{36}ClN_5OS$ [561.23].

4.5.12. 2-(Ethyl(6-(5,6,7,8-tetrahydroacridin-9-ylamino)hexyl) amino)-*N*-(4-phenylthiazol-2-yl)acetamide (9l)

Pale yellow oil, yield: 64%. Purity: 97.4%, t_R = 18.96 min. ^{1}H NMR ($CDCl_3$, 400 MHz, δ ppm): 10.52 (br s, 1H), 7.96 (d, J = 8.0 Hz, 1H), 7.92 (d, J = 8.4 Hz, 1H), 7.83 (d, J = 7.6 Hz, 2H), 7.56 (t, J = 7.6 Hz, 1H), 7.40 (t, J = 7.6 Hz, 2H), 7.32 (m, 2H), 7.14 (s, 1H), 4.06 (br s, 1H), 3.49 (t, J = 7.2 Hz, 2H), 3.29 (s, 2H), 3.08 (m, 2H), 2.68 (q, J = 7.2 Hz, 2H), 2.63 (m, 2H), 2.57 (t, J = 7.2 Hz, 2H), 1.89 (m, 4H), 1.70 (m, 2H), 1.53 (m, 2H), 1.42 (m, 4H), 1.12 (t, J = 7.2 Hz, 3H). ^{13}C NMR ($CDCl_3$, 100 MHz, δ ppm): 170.2, 157.6, 157.1, 151.1, 150.1, 143.3, 134.4, 128.7 (3C), 128.0 (2C), 126.0 (2C), 123.8, 122.9, 119.7, 116.4, 107.7, 57.5, 55.1, 49.3 (2C), 33.4, 31.7, 27.2 (2C), 26.8, 24.6, 22.9, 22.5, 12.0. ESI-MS $[M+H]^+$ (m/z): 542.3. $C_{32}H_{39}N_5OS$ [541.29].

4.5.13. 2-(Ethyl(6-(5,6,7,8-tetrahydroacridin-9-ylamino)hexyl) amino)-*N*-(4-(4-methoxyphenyl)thiazol-2-yl)acetamide (9m)

Pale yellow oil, yield: 61%. Purity: 99.1%, t_R = 17.67 min. ^{1}H NMR ($CDCl_3$, 400 MHz, δ ppm): 10.50 (br s, 1H), 7.91 (d, J = 8.4 Hz, 2H), 7.76 (d, J = 8.8 Hz, 2H), 7.54 (t, J = 8.4 Hz, 1H), 7.32 (t, J = 8.4 Hz, 1H), 7.00 (s, 1H), 6.92 (d, J = 8.8 Hz, 2H), 3.92 (br s, 1H), 3.82 (s, 3H), 3.46 (t, J = 7.2 Hz, 2H), 3.28 (s, 2H), 3.06 (m, 2H), 2.67 (q, J = 7.2 Hz, 2H), 2.66 (m, 2H), 2.56 (t, J = 7.2 Hz, 2H), 1.90 (m, 4H), 1.68 (m, 2H), 1.52 (m, 2H), 1.41 (m, 4H), 1.11 (t, J = 7.2 Hz, 3H). ^{13}C NMR ($CDCl_3$, 100 MHz, δ ppm): 170.3, 159.5, 158.3, 156.9, 150.7, 149.9, 147.4, 128.6, 128.3, 127.4, 127.3(2C), 123.6, 122.8, 120.2, 115.8, 114.1 (2C), 106.0, 57.5, 55.3, 55.1, 49.3, 49.2, 33.9, 31.7, 27.2, 27.1, 26.9, 24.7, 23.0, 22.7, 12.0. ESI-MS $[M+H]^+$ (m/z): 572.3. $C_{33}H_{41}N_5O_2S$ [571.3].

4.6. AChE and BuChE inhibition assay

Acetylcholinesterase (AChE, E.C. 3.1.1.7, from electric eel), butyrylcholinesterase (BuChE, E.C.3.1.1.8, from equine serum), 5,5′-dithiobis-(2-nitrobenzoic acid) (Ellman's reagent, DTNB), acetylthiocholine chloride (ATC), and butylthiocholinlrine chloride (BTC) were purchased from sigma. Synthesized derivatives were dissolved in DMSO and then diluted in PBS (pH 7.4) to provide a final concentration range. AChE enzyme solution was prepared to give 0.22 units/ml in 10 mL aliquots. The assay medium contained 20 μl PBS (pH 7.4), 20 μl compound solution or blank solution, 100 μl of 1.5 mM DTNB, 50 μl of enzyme, and 10 μl of 30 mM ATC. The assay medium containing 20 μl PBS (pH 7.4), 50 μl of enzyme, and 20 μl compound solution was allowed to incubate for 5 min, and then 100 μl of 1.5 mM DTNB were added for 5 min. The reaction was started by addition of 10 μl of 30 mM ATC. The activity was determined by measuring the increase in absorbance at 415 nm at 3 min intervals by a Biotek *ELx* 800 microplate reader. The similar method described above was applied to determine the BuChE activity (0.3 units/mL BuChE enzyme solution, 1.5 mM DTNB, 30 mM BTC).

4.7. Kinetic characterization of acetylcholinesterase inhibition

To obtain kinetic study on the mechanism of AChE inhibition by compound **7c**, reciprocal plots of 1/velocity versus 1/[substrate] were constructed at relatively low concentration of substrate (0.067–0.5 mM) by using Ellman's method. Three concentrations of compound **7c** were selected for this study: 20, 40, and 80 nm. The assay medium containing 20 μl PBS (pH 7.4), 50 μl of enzyme, and 20 μl compound solution was allowed to incubate for 5 min, and then 100 μl of 1.5 mM DTNB were added for 5 min. The reaction was started by addition of 10 μl different concentration of ATC. Kinetic characterization of the hydrolysis of ATC catalyzed by AChE was measured at 415 nm at 3 min intervals by a Biotek *ELx* 800 microplate reader.

4.8. Thioflavin T (ThT) fluorescence assay

$A\beta_{1-42}$ was dissolved in 100% 1,1,1,3,3,3-hexafluoro-2-propanal (HFIP) to a concentration of 1 mg/mL, sonicated in a water bath for 10 min, aliquoted into microcentrifuge tubes, dried under vacuum, and stored at −20 °C. Immediately prior to use, the HFIP-treated $A\beta_{1-42}$ was dissolved in dimethylsulfoxide (DMSO) as the stored solution. A screening assay for all compounds that inhibited $A\beta_{1-42}$ aggregation was performed by measuring the ThT fluorescence emission. Amounts of 5 μl compound (200 μM) and 5 μl of 200 μM $A\beta_{1-42}$ were added into 40 μl of phosphate-buffered saline (PBS at pH 7.4). After incubation for 24 h at room temperature, 100 μl of 5 μM ThT solution (in PBS at pH 7.4) was added to the reaction solution. Fluorescence was measured at 485 nm with an excitation wavelength of 435 nm on a perkinelmer LS-55 fluorospectrophotometer.

4.9. Atomic force microscopy (AFM) assay

The HFIP-treated $A\beta_{1-42}$ was dissolved in DMSO to 2 mM as stock solution. Phosphate buffer (PBS) was dissolved by milliporewater, and filtered by 0.22 μM microfiltration membrane. $A\beta_{1-42}$ (1 mM, 2.5 μl), PBS (pH 7.4, 45 μl), and 9 m (2 mM, 2.5 μl) were incubated for 4 days at 30 °C. As a control, 2 mM $A\beta_{1-42}$ (2.5 μl), PBS (pH 7.4, 45 μl), and DMSO (2.5 μl) were incubated for 4 days at 30 °C. AFM experiments were performed as follows: Take an aliquot of 10 μl from the incubating solution and deposit it on the mica surface directly. The deposited droplet is left on the mica surface for 10 min and wash the sample with ultra-pure water to remove excess salts and unbound peptide. Gently blow the sample dry under a stream of nitrogen. Finally, scan samples with tapping mode on a PicoScan 2500 PicoSPM II controller with a silicon probe of k = 40 N/m and 300 kHz resonant frequency.

4.10. Cell culture of rat cortical neurons

Neonatal Sprague-Dawley (SD) rats (day 0–3) were obtained from the Experimental Animal Center of Tongji Medical College, Huazhong University of Science & Technology. All experiments conformed to the local and international guidelines on ethical use of animals. The University Animal Welfare Committee approved the used animal protocol. Briefly, the cortex of newborn SD rats were dissected and rinsed in ice-cold Dulbecco's phosphate-buffered saline. The dissected tissues were treated with 0.125% trypsin in Hanks' balanced salt solution for 25 min at 37 °C and mechanically dissociated using a fire-polished Pasteur pipettes. Cells were collected by centrifugation and resuspended in DMEM/F12 (1:1) with 10% fetal bovine serum. For calcium imaging, cells (20,000–40,000) were seeded on poly-D-lysine coated coverslips and kept at 37 °C in 5% CO_2 incubator. After 24 h, the culture medium was changed into DMEM medium supplemented with 2% B27 and the cortical neurons were fed with fresh medium twice weekly. Microscopically, glial cells were not apparent by employing this protocol. The neurons were main-

tained for 6–8 d in primary culture until used for calcium imaging.

4.11. Calcium imaging assay

The cells were washed three times with artificial cerebrospinal fluid (ACSF) containing (in mM): 140 NaCl, 5 KCl, 1 $MgCl_2$, 2 $CaCl_2$, 10 glucose, and 10 HEPES (pH 7.3), loaded with 1 μM Fura-2/AM in ACSF for 40 min at 37 °C, and then washed with ACSF to remove the excess extracellular Fura-2/AM. Coverslips were mounted on a chamber positioned on the movable stage of an inverted microscope (TE2000, Japan), which is equipped with a calcium imaging system (PTI, USA). Fluorescence was excited at wavelengths of 340 nm for 150 ms and 380 nm for 50 ms at 1 s interval by a monochromator (PTI K-178-S) and the emitted light was imaged at 510 nm with a video camera (CoolSNAP HQ2, ROPPER, USA) through fluor oil-immersion lens (Nikon X-70) and a wide band emission filter. The F340/F380 fluorescence ratio was recorded and analyzed by MetaFluor version 6.3 software. The F340/F380 fluorescence ratio was used as an indicator of Ca^{2+} concentration. Data are mean ± SEM of at least three different cell cultures.

Acknowledgments

This work was supported by Grants from the Key Project of National Natural Science Foundation of China (No.30930104), International Science & Technology Cooperation Program of China (No. 2011DFA32670) and the Important National Science & Technology Specific Projects (No. 2012ZX09103-101-045) to Dr. J.G Chen.

Supplementary data

Supplementary data associated with this article can be found, in the online version, at http://dx.doi.org/10.1016/j.bmc.2012.08.040. These data include MOL files and InChiKeys of the most important compounds described in this article.

References and notes

1. Querfurth, H. W.; LaFerla, F. M. *N. Eng. J. Med.* **2010**, *362*, 329.
2. Citron, M. *Nat. Rev. Drug Disc.* **2010**, *9*, 387.
3. Walsh, D. M.; Selkoe, D. J. *Neuron* **2004**, *44*, 181.
4. McLean, C. A.; Cherny, R. A.; Fraser, F. W.; Fuller, S. J.; Smith, M. J.; Beyreuther, K.; Bush, A. I.; Masters, C. L. *Ann. Neurol.* **1999**, *46*, 860.
5. Naslund, J.; Haroutunian, V.; Mohs, R.; Davis, K. L.; Davies, P.; Greengard, P.; Buxbaum, J. D. *JAMA* **2000**, *283*, 1571.
6. Estrada, L. D.; Soto, C. *Curr. Top. Med. Chem.* **2007**, *7*, 115.
7. Rampa, A.; Belluti, F.; Gobbi, S.; Bisi, A. *Curr. Top. Med. Chem.* **2011**, *11*, 2716.
8. Hopkins, A. L. *Nat. Chem. Biol.* **2008**, *4*, 682.
9. Cavalli, A.; Bolognesi, M. L.; Minarini, A.; Rosini, M.; Tumiatti, V.; Recanatini, M.; Melchiorre, C. *J. Med. Chem.* **2008**, *51*, 347.
10. Huang, L.; Su, T.; Shan, W.; Luo, Z.; Sun, Y.; He, F.; Li, X. *Bioorg. Med. Chem.* **2012**, *20*, 3038.
11. Wang, Y.; Guan, X. L.; Wu, P. F.; Wang, C. M.; Cao, H.; Li, L.; Guo, X. J.; Wang, F.; Xie, N.; Jiang, F. C.; Chen, J. G. *J. Med. Chem.* **2012**, *55*, 3588.
12. Camps, P.; Formosa, X.; Galdeano, C.; Muñoz-Torrero, D.; Ramírez, L.; Gómez, E.; Isambert, N.; Lavilla, R.; Badia, A.; Clos, M. V.; Bartolini, M.; Mancini, F.; Andrisano, V.; Arce, M. P.; Rodríguez-Franco, M. I.; Huertas, O.; Dafni, T.; Luque, F. J. *J. Med. Chem.* **2009**, *52*, 5365.
13. Luo, W.; Li, Y. P.; He, Y.; Huang, S. L.; Tan, J. H.; Ou, T. M.; Li, D.; Gu, L. Q.; Huang, Z. S. *Bioorg. Med. Chem.* **2011**, *19*, 763.
14. Fang, L.; Jumpertz, S.; Zhang, Y.; Appenroth, D.; Fleck, C.; Mohr, K.; Tränkle, C.; Decker, M. *J. Med. Chem.* **2010**, *53*, 2094.
15. Marco-Contelles, J.; León, R.; de Los Ríos, C.; Guglietta, A.; Terencio, J.; López, M. G.; García, A. G.; Villarroya, M. *J. Med. Chem.* **2006**, *49*, 7607.
16. Marco-Contelles, J.; León, R.; de los Ríos, C.; Samadi, A.; Bartolini, M.; Andrisano, V.; Huertas, O.; Barril, X.; Luque, F. J.; Rodríguez-Franco, M. I.; López, B.; López, M. G.; García, A. G.; Carreiras Mdo, C.; Villarroya, M. *J. Med. Chem.* **2009**, *52*, 2724.
17. Pickhardt, M.; Larbig, G.; Khlistunova, I.; Coksezen, A.; Meyer, B.; Mandelkow, E. M.; Schmidt, B.; Mandelkow, E. *Biochemistry* **2007**, *46*, 10016.
18. Bulic, B.; Pickhardt, M.; Schmidt, B.; Mandelkow, E. M.; Waldmann, H.; Mandelkow, E. *Angew. Chem., Int. Ed.* **2009**, *48*, 1740.
19. Ohkubo, M.; Kuno, A.; Nakanishi, I.; Takasugi, H. *Chem. Pharm. Bull.* **1995**, *43*, 1497.
20. Panico, A. M.; Geronikaki, A.; Mgonzo, R.; Cardile, V.; Gentile, B.; Doytchinova, I. *Bioorg. Med. Chem.* **2003**, *11*, 2983.
21. Zhang, W. T.; Ruan, J. L.; Wu, P. F.; Jiang, F. C.; Zhang, L. N.; Fang, W.; Chen, X. L.; Wang, Y.; Cao, B. S.; Chen, G. Y.; Zhu, Y. J.; Gu, J.; Chen, J. G. *J. Med. Chem.* **2009**, *52*, 718.
22. Fang, L.; Appenroth, D.; Decker, M.; Kiehntopf, M.; Lupp, A.; Peng, S.; Fleck, C.; Zhang, Y.; Lehmann, J. *J. Med. Chem.* **2008**, *51*, 7666.
23. Ellman, G. L.; Courtney, K. D.; Andres, B. J.; Featherstone, R. M. *Biochem. Pharmacol.* **1961**, *7*, 88.
24. Darvesh, S.; Hopkins, D. A.; Geula, C. *Nat. Rev. Neurosci.* **2003**, *4*, 131.
25. Greig, N. H.; Utsuki, T.; Yu, Q.; Zhu, X.; Holloway, H. W.; Perry, T. A.; Lee, B.; Ingram, D. K.; Lahiri, D. K. *Curr. Med. Res. Opin.* **2001**, *17*, 159.
26. Furukawa-Hibi, Y.; Alkam, T.; Nitta, A.; Matsuyama, A.; Mizoguchi, H.; Suzuki, K.; Moussaoui, S.; Yu, Q.-S.; Greig, N. H.; Nagai, T.; Yamada, K. *Behav. Brain Res.* **2011**, *225*, 222.
27. Biancalana, M.; Koide, S. *Biochim. Biophys. Acta* **2010**, *1804*, 1405.
28. Legleiter, J. *Methods Mol. Biol.* **2011**, *670*, 57.
29. Bezprozvanny, I.; Mattson, M. P. *Trends Neurosci.* **2008**, *31*, 454.
30. LaFerla, F. M. *Nat. Rev. Neurosci.* **2002**, *3*, 862.